

Evaluation of the frequency stability of a VCSEL locked to a micro-fabricated Rubidium vapour cell

J. Di Francesco, F. Gruet, C. Schori, C. Affolderbach, R. Matthey, G. Mileti
Laboratoire Temps – Fréquence (LTF), Institute of Physics
University of Neuchâtel, Avenue de Bellevaux 51, CH – 2009 Neuchâtel, Switzerland

Y. Salvadé
Laboratory of Metrology and Quality Engineering, University of Applied Sciences, Haute Ecole Arc
Ingénierie, St-Imier, Switzerland

Y. Petremand, N. De Rooij
Ecole Polytechnique Fédérale de Lausanne (EPFL), Sensors, Actuators and Microsystems
Laboratory, Rue Jaquet-Droz 1, 2000 Neuchâtel, Switzerland

ABSTRACT

We present our evaluation of a compact laser system made of a 795 nm VCSEL locked to the Rubidium absorption line of a micro-fabricated absorption cell. The spectrum of the VCSEL was characterised, including its RIN, FM noise and line-width. We optimised the signal-to-noise ratio and determined the frequency shifts versus the cell temperature and the incident optical power. The frequency stability of the laser (Allan deviation) was measured using a high-resolution wavemeter and an ECDL-based reference. Our results show that a fractional instability of $\leq 10^{-9}$ may be reached at any timescale between 1 and 100'000 s. The MEMS cell was realised by dispensing the Rubidium in a glass-Silicon preform which was then, sealed by anodic bonding. The overall thickness of the reference cell is 1.5 mm. No buffer gas was added. The potential applications of this compact and low-consumption system range from optical interferometers to basic laser spectroscopy. It is particularly attractive for mobile and space instruments where stable and accurate wavelength references are needed.

Keywords: Vertical cavity surface emitting laser (VCSEL), micro-fabricated absorption cell, Rubidium, laser frequency stabilization, Allan deviation, spectroscopy

1. INTRODUCTION

Stabilization of the output frequency of a semiconductor laser source [1] to reference etalons [2] or atomic reference lines [3, 4] has become a well-established tool in a wide field of research topics, and is also implemented in applications such as, e.g., atomic clocks and atomic magnetometers [5], interferometry [6], and wavelengths references [7].

In this paper, we investigate the frequency stability of a new frequency standard composed of a vertical-cavity surface-emitting laser (VCSEL) locked to a Doppler-broadened absorption resonance on the D1 line of atomic ^{85}Rb , using either a micro-fabricated or a traditional cm-scale glass vapour cell. VCSEL diode lasers have the advantages of low power consumption, intrinsic mode-hop free single-mode operation, and a good potential for cost-effective mass production, making them ideal candidates for the realization of a compact, stabilized wavelength source. The Rb absorption line obtained from the vapour cell serves as a reference with good long-term stability, thanks to its small frequency shifts in response to external fields and operating conditions [8]. Recently, progress of silicon machining and anodic-bonding have resulted in the creation of micro-fabricated absorption cells filled with alkali vapour that allow a more radical miniaturization of the whole setup. Similar laser frequency stabilization techniques are employed in micro-fabricated atomic clocks and magnetometers [5], but not detailed studies of the obtained laser frequency stability have been published.

2. EXPERIMENTS

2.1 Experimental setup

We use a VCSEL laser diode emitting around 795 nm, operated at a temperature of 59.5°C and an injection current of 1.97 mA. Optical feedback on the VCSEL is limited thanks to the use of an optical isolator and an antireflection (AR) coating for the lens which collimated the laser beam (not show in Figure 1). After passing through the Rb vapour cell, the transmitted light power in the laser beam is detected on a Si photodiode detector.

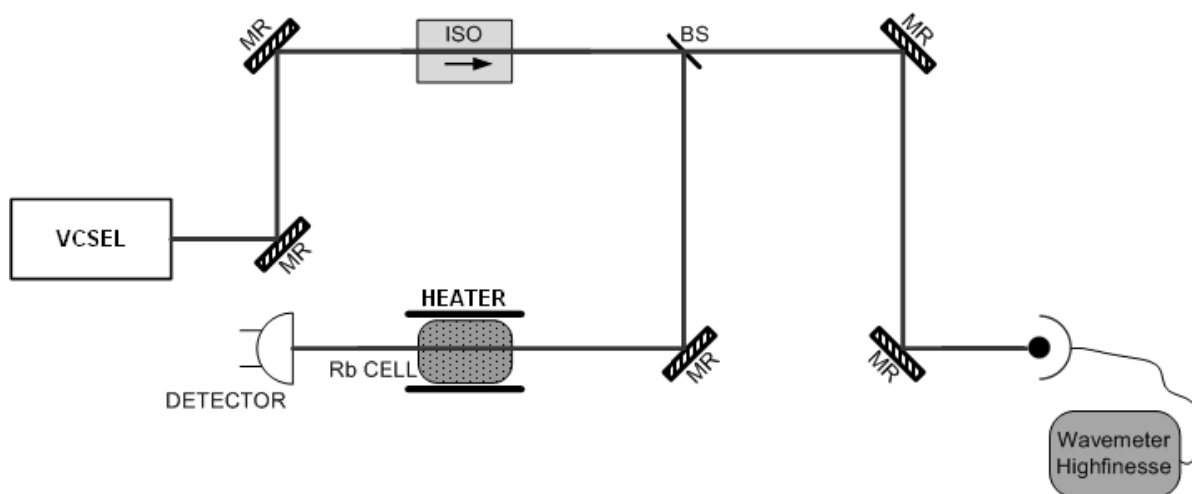


Figure 1 – Experimental setup: frequency stability is measured using a high precision wavemeter. ISO = optical isolator, MR = mirror, BS = beam splitter.

Laser stabilization to two cells with different sizes is studied, using the same setup and similar conditions. One cell is a traditional cylindrical glass cell with 10 mm diameter and 20 mm length and the second cell is a 1.5 mm thick micro-fabricated cell (see section 2.2). Both cells contain atomic Rubidium in natural isotope mixture. The Rubidium vapour density at room temperature is low for both cells resulting in too weak absorption signals. To increase the DC signal the micro-fabricated and cm-scale glass cells are heated to 90 °C and 55 °C, respectively. The cell temperature is stabilised by a feed-back regulated thermostat. The typical optical power incident to the cell is 250 μ W and the beam diameter is 1.4 mm.

The error signal for laser frequency stabilization is obtained by modulation of the VCSEL current at 50 kHz and using 1f lock-in detection. The VCSEL frequency measurement is measured with a high precision wavemeter (High-Finesse type WSU/2). In a typical measurement run the frequency is recorded each 0.15 second during one day. To improve the measurement quality all the setup is placed under an opaque box which protects to against temperature fluctuations and changes in background light in the test room.

2.2 MEMS Cell fabrication

The main steps of the vapour cells fabrication technology is described in Figure 2. First, a silicon wafer is prepared for cavity etching by photolithography. For this step, a silicon dioxide is grown on the surface. Then, after photolithography,

the wafer is etched by DRIE (Deep Reactive Ion Etching) etching in order to obtain through holes of the desired dimension. The obtained hollowed wafer is then bonded to a glass (borofloat) wafer by anodic bonding. The obtained bonded wafers are then diced to obtain preforms. In parallel, a glass wafer is diced to form glass lids of the same dimension than the preforms. From this point, the fabrication is continued at chip level.

The obtained chips (preform and lid) are placed into the deposition machine as seen in Figure 3. The chamber is closed and a high vacuum is made inside the chamber. The preform, placed on a movable trolley is displaced to the Rb dispensing position, below a system based on a commercially available Rb dispenser from SAES getters. Once a small amount of Rb is deposited into the preform cavity, the preform is moved to the bonding position, below the glass lid. The lid, mounted on a piston, is finally moved in contact to the Rb filled preform to close the cavity and obtain a hermetic sealing of the chip by anodic bonding. The anodic bonding technique is based on the work of Wallis and Pomerantz and includes the following process; once the silicon preform and the glass lid are in contact at a given pressure, the system is heated up to about 300 °C and a voltage of 600 V or more is applied between the glass lid and the silicon preform. At that temperature, the sodium ions within the borosilicate glass matrix become mobile and can be moved by the negative bonding voltage. A depletion zone is created in which a voltage drop occurs. This effect creates a large electrostatic force enabling a mechanical contact on the atomic scale between the two surfaces to be bonded. By field-assisted oxygen ion diffusion, an anodic oxidation forms a very strong bond between the glass and the silicon surfaces.

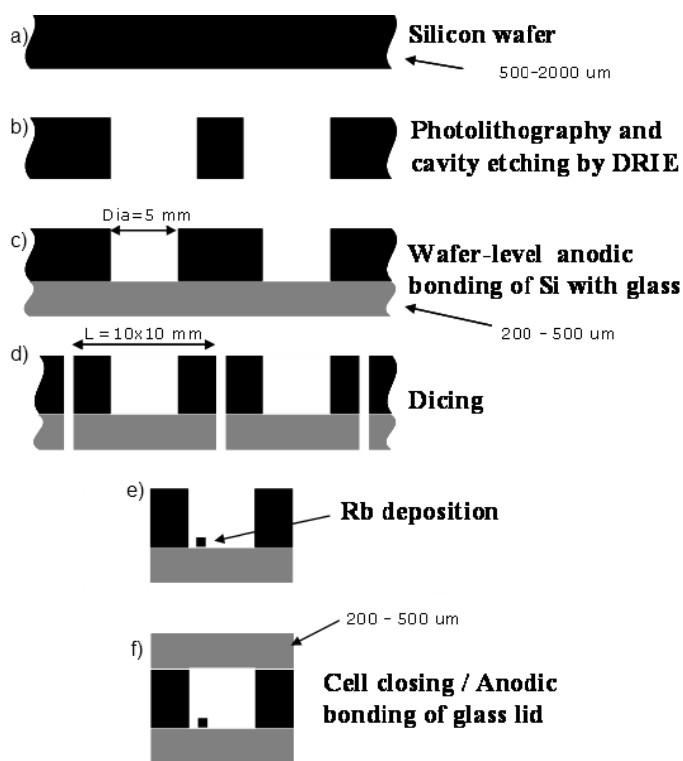


Figure 2 – Process flow of the cell fabrication (cross section view). a) Preparation of a silicon wafer (500, 1000, 1500 or 2000 μm thick). b) Photolithography and cavity etching by DRIE. c) Wafer-level anodic bonding of the Si wafer with a glass wafer. d) Dicing of the obtained preform. e) Silicon surface preparation and Rb deposition in the cavity. f) Cell bonding with a glass lid by anodic bonding.

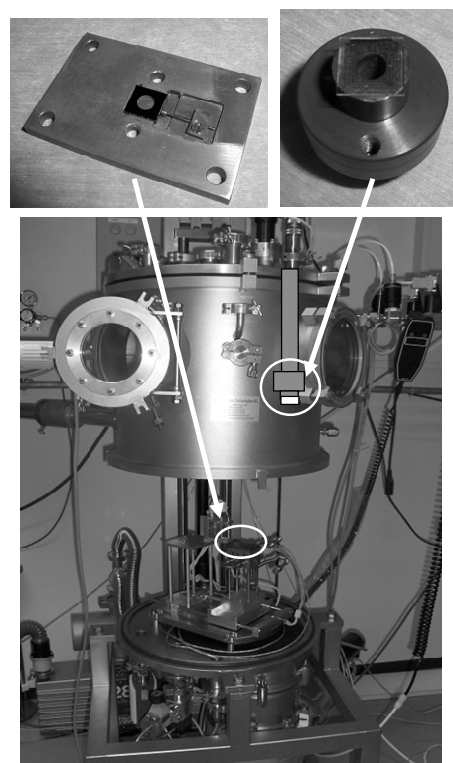


Figure 3 – Picture of the Rb deposition and cell closing machine. The glass lid (upper right corner) is installed on a vertically movable system while the preform (upper left corner) is mounted on a horizontally movable carrier

2.3 Laser properties

The VCSEL laser source is from Avalon¹, emitting around 795 nm. To achieve laser emission on the D1 line of Rubidium, the VCSEL is operated at 59.5 °C and 1.97 mA. At this operating point the total output power is 0.25 mW while the current and temperature tuning coefficients are -122.4 GHz/mA and -31.8 GHz/K, respectively (Figure 4). We have measured the frequency noise spectrum shown in Figure 5, using a discriminator slope of the ⁸⁵Rb line (F=3). The density of frequency fluctuations at 1 kHz is approximately $2.5 \cdot 10^9 \text{ Hz}^2/\text{Hz}$. The VCSEL linewidth was measured to be $45 \pm 3 \text{ MHz}$, from a beat measurement against an extended-cavity diode laser (ECDL) having a linewidth of 200 kHz. This result was confirmed in a second measurement using a Fabry-Pérot interferometer with a resolution of 1 MHz.

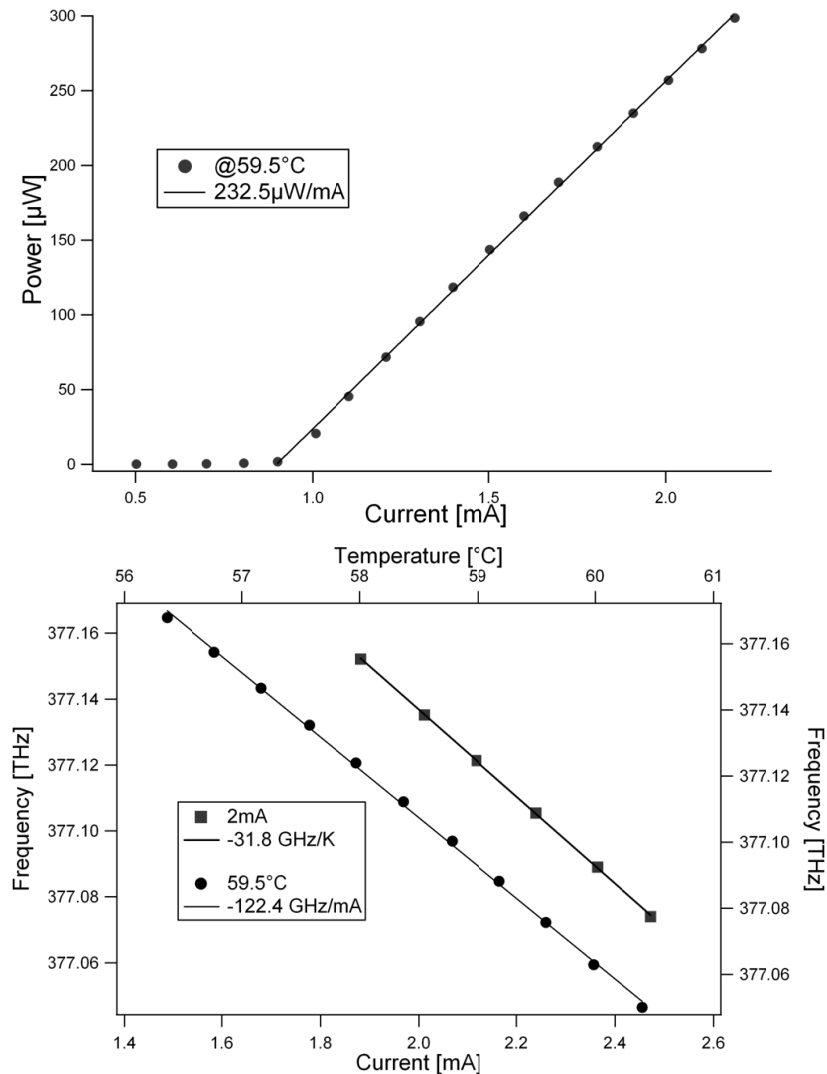


Figure 4 – PI curve and tuning coefficients.

¹ For this work we used a 795nm single-mode VCSEL from Avalon Photonics (now Bookham Inc.), emitting at 795nm. However, this choice is not critical for the results reported here, and similar results can be expected when using a single-mode VCSEL from other manufacturers. In particular, we also evaluated 795nm single-mode VCSEL from ULM Photonics (type 795-01-TN-S46FOP), and found similar laser characteristics as the ones reported here for the Avalon device.

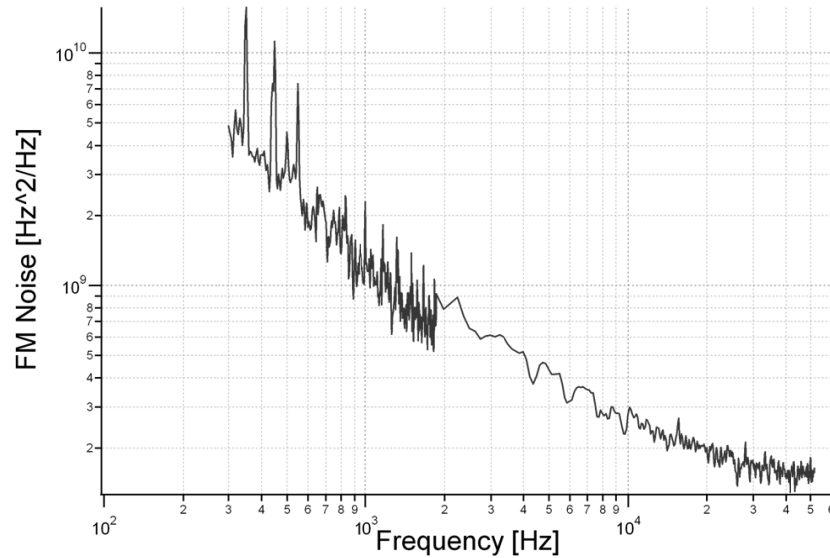


Figure 5 – Frequency noise spectrum of the VCSEL when operated at a temperature of 59.5 °C and a current of 2 mA.

2.4 Frequency stability

In a first step, we calculated the theoretical short-term frequency stability - in terms of Allan Deviation [9] - that can be obtained with our setup. Equation (1) gives the theoretical limit which is expressed in terms of the detection noise power spectral density N_{PSD} measured on the detector behind the Rb cell, the discriminator slope D and the VCSEL frequency ν_{VCSEL} [10]:

$$\sigma_{th}(\tau) = \frac{N_{PSD}}{\sqrt{2} \cdot \nu_{VCSEL} \cdot D} \cdot \tau^{-\frac{1}{2}} \quad (1)$$

D is obtained from a linear fit to the error signal close to its zero crossing. Figure 6 shows an example of the DC transmission signal through the cell (black trace) and the corresponding error signal (grey trace) obtained by scanning the VCSEL frequency across the Rubidium D1 absorption line.

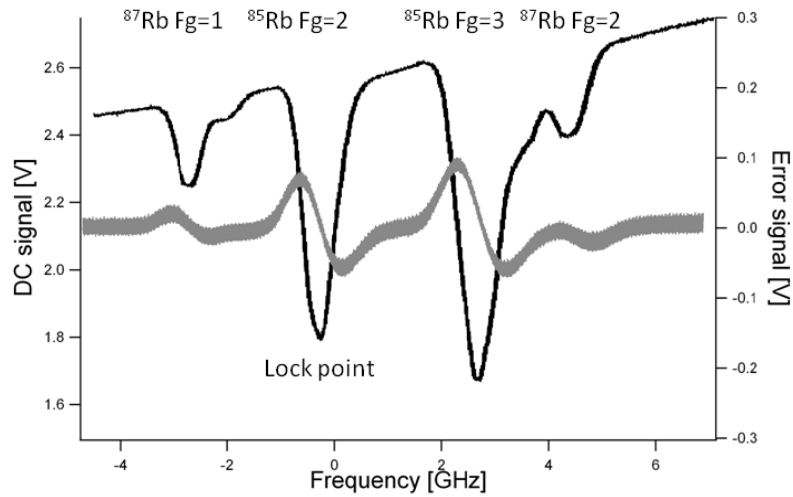


Figure 6 – Absorption and error signal for the micro-fabricated cell.

Parameter	Unit	cm-scale glass cell	μ -fabricated cell
Discriminator	V/GHz	3.26	1.83
Detection noise PSD	mVrms/sqrt(Hz)	0.768	0.431
Theoretical frequency stability	$\tau^{-1/2}$	$4.41 \cdot 10^{-10}$	$5.04 \cdot 10^{-10}$

Table 1 – Short-term frequency stability prediction according to equation (1).

Figure 7 shows the measured fractional frequency stability of the stabilized VCSEL (in term of Allan deviation) as a function of averaging time. First, we can see that the theoretical estimations of for the short-term laser stability given in Table 1 and the experimental values are perfectly matched, up to integration times of $\tau = 10$ s. Furthermore, there is only a small difference between the stabilities obtained with two cells, the cm-scale glass cell giving a slightly better short-term stability. From 10 seconds the measured Allan Deviation increases with the same tendency for both cells, due to a long-term drift of the wavemeter used. This is confirmed by a separate measurement of a highly stable laser source (ECDL) [3], achieving $\sigma_{ECDL}(\tau) \leq 10^{-12}$ on all time scales considered here. This measurement confirms the wavemeter resolution being $\sigma_{WM}(\tau) \approx 2 \cdot 10^{-10}$ at $\tau = 1$ s, and its stability $\sigma_{WM}(\tau) \approx 1 \cdot 10^{-9}$ at $\tau = 1000$ s.

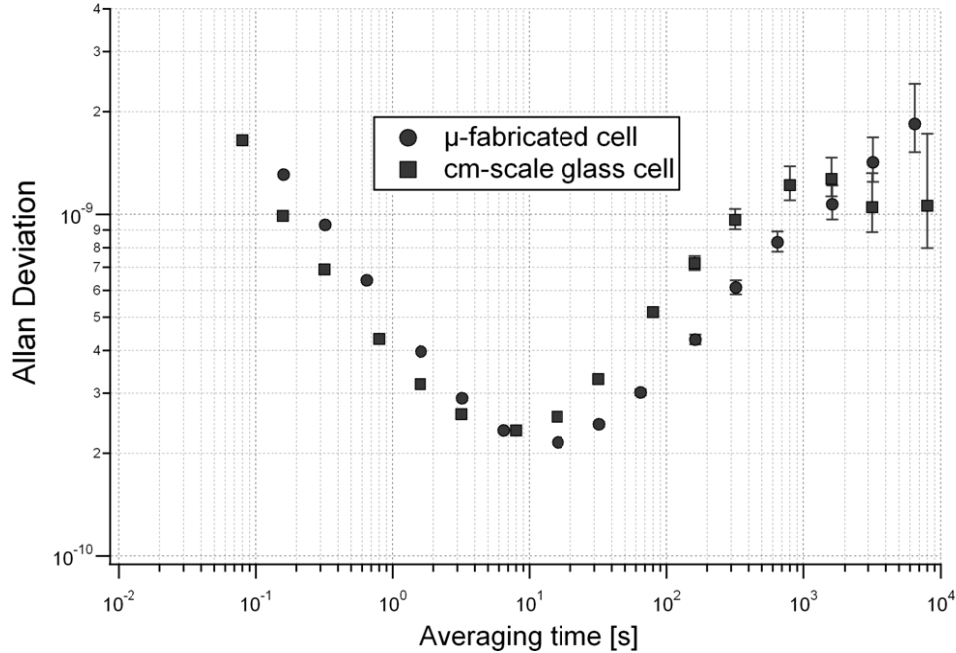


Figure 7 – Relative frequency stability of the VCSEL frequency stabilized to the two Rb cells, in terms of the Allan Deviation.

2.5 Frequency shift versus cell temperature and the incident optical power

Two main sources of systematic frequency shifts have to be taken into account when stabilizing to Doppler-broadened Rb absorption lines [8]: the cell temperature and the optical power incident on the cell. These factors may well limit the observed frequency stability and therefore their impact on the stabilized laser frequency was measured. In a first step, the cell temperature was varied by $\pm 1^\circ\text{C}$ around the operating point. In a second step, the optical power was varied by a few μW around the operating point. In both cases, the resulting frequency shift was measured with the wavemeter. The results are shown in Table 2.

Cell	Shifts according to the cell temperature	Shifts according to the incident optical power
cm-scale	$0.6 \text{ MHz}/^\circ\text{K} \pm 1 \text{ MHz}/^\circ\text{K}$	$< 200 \text{ kHz}/\mu\text{W}$
Micro-fabricated	$1 \text{ MHz}/^\circ\text{K} \pm 1 \text{ MHz}/^\circ\text{K}$	$< 200 \text{ kHz}/\mu\text{W}$

Table 2 – Shift of the stabilized laser frequency in response to changes in experimental parameters.

The temperature stability of the Rb cells at 10^4 seconds is approximately 10 mK, leading to a frequency shift of 10 kHz for the Rb reference line. This shift contributes an amount $\sigma_{\text{VCSEL}} \approx 3 \times 10^{-11}$ to the fractional frequency instability of the VCSEL. The typical fractional instability of the optical power is $< 6 \times 10^{-4}$ at 10^4 s, which corresponds to a laser frequency instability contribution of $\sigma_{\text{VCSEL}} \approx 8 \times 10^{-11}$. The fluctuations in optical power present the most important limitation to the laser stability reported here. In total, we expect the frequency instability to be limited to $\sigma_{\text{VCSEL}} \leq 9 \times 10^{-11}$ at $\tau = 10^4$ s, which is however not resolved in our experiment due to the insufficient stability of the wavemeter.

3. CONCLUSIONS

Our results show that Doppler-broadened Rb absorption lines obtained from micro-fabricated vapour cells of mm-scale dimensions can be used to stabilize the frequency of a VCSEL diode laser to the level of $\sigma_{\text{VCSEL}} = 5 \times 10^{-10}$ at $\tau=1$ s. This stability is essentially the same as obtained with a classical cm-scale vapor cell and could be obtained in spite of the relatively large emission linewidth of the VCSEL. Our stability results compare well to the stabilities reported or predicted for similar schemes, but without the need for stringent requirements on cell thickness and diameter [11, 12] or additional pump laser beams [13, 14]. The simplicity of the used setup and small size of the few key components used opens the way for the realization of a low-power frequency-stabilized laser source with an overall physics package volume of only a few cm^3 .

We finally note that we observed similar frequency stability as reported above also for a VCSEL laser emitting at 780nm, stabilized to the Rb D2 absorption lines obtained from the same cells. This extends the wavelength range of the stabilized laser, without need to change the reference cell.

4. OUTLOOK AND APPLICATIONS POTENTIALS

Already with its present stability performance, the demonstrated frequency-stabilized VCSEL laser is appropriate for applications in miniaturized precision instrumentation requiring a stabilized frequency reference, such as, e.g., atomic clocks and atomic magnetometers [5]. Further improvement in short-term frequency stability may be expected when stabilizing the VCSEL to Doppler-free saturated-absorption lines that still can be resolved in spite of the relatively large VCSEL linewidth [12, 14]. Preliminary experiments on saturated-absorption lines observed with our setup show that the short-term frequency stability reaches $\sigma_{\text{VCSEL}} = 2 \times 10^{-10}$ at $\tau=1$ s, which coincides with the resolution limit of the wavemeter used.

5. ACKNOWLEDGEMENTS

We acknowledge financial support from the Swiss National Science Foundation (Subsidy 200020-118162 and Sinergia program grant no. CRSI20_122693/1), the European Space Agency (ESTEC contracts 20794/07/NL/GLC and 19392/05/NL/CP), and the Swiss Space Office. We thank P. Scherler (LTF) for technical support.

REFERENCES

- [1] Hall, J. L., Taubman, M. S., and Ye, J., "Laser stabilization", in : [Handbook of optics], vol.4, 2nd edition, McGraw-Hill, New York (2000).
- [2] Drever, R. W. P., Hall, J. L., Kowalski, F. V., Hough, J., Ford, G. M., Munley, A. J., and Ward, A., "Laser Phase and Frequency Stabilization Using an Optical Resonator", *Appl. Phys. B* 31, 97 – 105, (1983).
- [3] Affolderbach, C., and Mileti, G., "A compact laser head with high-frequency stability for Rb atomic clocks and optical instrumentation," *Rev. Sci. Instrum.* 76, 073108, (2005).
- [4] Ye, J., Swartz, S., Jungner, P., and Hall, J. L., "Hyperfine structure and absolute frequency of the ^{87}Rb $5P_{3/2}$ state", *Opt. Lett.* 21(16), 1280 – 1282, (1996).
- [5] Knappe, S., Schwindt, P. D. D., Gerginov, V., Shah, V., Liew, L., Moreland, J., Robinson, H. G., Hollberg, L., and Kitching, J., "Microfabricated Atomic Clocks and Magnetometers", *J. Opt. A* 8, S318 – S322, (2006).
- [6] Salvadé, Y. and Dändliker, R., "Limitations of interferometry due to the flicker noise of laser diodes", *J. Opt. Soc. Am. A* 17(5), 927 - 932 (2000).
- [7] Têtu, M., Cyr, N., Villeneuve, B., Thériault, S., Breton, M., and Tremblay, P., "Towards the Realization of a Wavelength Standard at 780nm Based on a laser diode Frequency Locked to Rubidium Vapor", *IEEE Trans. Instrum. Meas.* 40(2), 191 - 195, (1991).

- [8] Affolderbach, C., Mileti, G., Slavov, D., Andreeva, C., and Cartaleva, S., “Comparison of simple and compact Doppler and sub-Doppler laser frequency stabilization schemes”, Proceedings of the 18th European Frequency and Time Forum (EFTF), The Institution of Electrical Engineers, London, paper 084 (2004).
- [9] Allan, D. W., “Time and Frequency (Time-Domain) Characterization, Estimation, and Prediction of Precision Clocks and Oscillators,” IEEE Trans. Ultrason., Ferroelec. Freq. Contr. 34(6), 647 - 654 (1987).
- [10] Mileti, G. and Thomann, P., “Study of the S/N Performance of Passive Atomic Clocks using a Laser Pumped Vapor”, Proceedings of the 9th European Frequency and Time Forum, Société Française des Microtechniques et de Chronométrie, Besançon, 271 - 276, (1995)
- [11] Zhao, Y. T., Zhao, J. M., Huang, T., Xiao, L. T., and Jia, S. T., “Frequency stabilization of an external-cavity diode laser with a thin Cs vapour cell”, J. Phys. D 37, 1316 – 1318 (2004).
- [12] Fukuda, K., Tachikawa, M., and Kinoshita, M., “Allan-variance measurements of diode laser frequency-stabilized with a thin vapor cell”, Appl. Phys. B 77, 823 – 827 (2003).
- [13] Knappe, S. A., Robinson, H. G., and Hollberg, L., “Microfabricated saturated absorption laser Spectrometer”, Opt. Express 15(10), 6293 – 6299 (2007).
- [14] Affolderbach, C., Nagel, A., Knappe, S., Jung, C., Wiedenmann, D., and Wynands, R., “Nonlinear Spectroscopy with a Vertical-Cavity Surface-Emitting Laser (VCSEL)”, Appl. Phys. B 70, 407 – 413 (2000).